Bearing Fault Diagnosis using Singular Spectrum Analysis-Based Envelope Detection

Guicai Zhang, Yun Li, and Changle Li

United Technologies Research Center (China), Shanghai 201204, P. R. China

ZhangG@utrc.utc.com
LiY2@utrc.utc.com
LiCL@utrc.utc.com

ABSTRACT

Rolling element bearings are critical components in rotating machinery and it is important to monitor their health and detect their faults in early stage during their operations. The vibration energy generated by the faults in rolling element bearings is usually small comparing to that of other rotating components such as rotors/shafts and gears in mechanical systems. Envelope analysis is a widely used method in bearing fault diagnosis. The major challenge in envelope analysis is the identification of resonance frequency band for narrow-band filtering before applying envelope operation. In this paper, a method combining singular spectrum analysis (SSA) and envelope analysis is proposed for diagnosing the rolling element bearing faults. The SSA is utilized to decompose the bearing vibration signal into a set of eigentriples (principle components), and then a subset of the eigentriples that encompass the dominant variation in the original signal is selected for signal reconstruction. Envelope analysis is then applied to the reconstructed signal to extract the modulation information that caused by the bearing faults. The proposed SSA-based envelope analysis is applied to the data sets of the bearing data center at Case Western Reserve University (CWRU), and the results are compared with that of the widely used Kurtogram-based envelope analysis. The results show that the SSA-based envelope analysis is more effective than the Kurtogram-based envelope analysis in bearing fault diagnosis.

1. INTRODUCTION

Rolling element bearings are the most widely used components in rotating machinery. Condition monitoring and fault diagnosis of rolling element bearings are important in the practice of equipment maintenance in industries. The vibration energy generated by the faults in rolling element bearings is usually small comparing to that of other rotating components such as rotors/shafts and gears in mechanical systems, especially for the faults in early stage. Envelope analysis is a powerful technique to detect faults in rolling element bearings. The resonance frequency band identification is the key for narrow-band filtering before applying envelope operation (Randall, 2011). In the past over twenty years, researchers put forwarded some methods for identifying the resonance frequency band, such as Kurtogram (Antoni & Randall, 2006), wavelet transform (Shi, Wang & Qu, 2004), etc. These methods are mainly based on spectral kurtosis evaluation of the frequency bands, i.e., using kurtosis as the criteria to determine the resonance frequency band. In some of the cases, the variance of the identified frequency band could be too small and the results of the envelope become meaningless and ineffective.

Singular spectrum analysis (SSA) is a non-parametric time series modeling technique and it is a relatively new technique for time series analysis (Broomhead & King, 1986). The main idea of SSA is to perform singular value decomposition (SVD) of the trajectory matrix obtained from the original time series with a subsequent reconstruction of the series. The advantage of SSA over Fourier analysis is that SSA components are not necessarily harmonic functions, being data adaptive and can capture highly nonharmonic oscillatory shapes. These advantages make SSA suitable for the analysis of nonlinear and non-stationary time series. SSA provides estimates of the statistical dimension and it also describes the main physical phenomena reflected by the data. It gives adaptive spectral filters associated with the dominant oscillations of the system and clarifies the noise characteristics of the data (Vautard & Ghil, 1989). SSA can decompose the original time series into the sum of a small number of independent and interpretable components such as slowly varying trend, oscillatory components and structureless noise (Hassani, 2010). It is a powerful tool for change detection, signal and noise separation, trend extraction, etc. In recent years, SSA has found applications including time series forecasting (Golyandina & Korobeynikov, 2014), signal and noise separation (Khelifa, Kahlouche, & Belbachir, 2012),

biomedical signal processing (Sanei & Hassani, 2016), manufacturing process monitoring (Salgado & Alonso, 2006; Kilundu, Dehombreux & Chiementin, 2011). It is also applied to structural health monitoring and mechanical fault diagnosis in very recent years. Zhao and Ye used SSA to diagnose headstock fault (2011). Liu, Chen and Dong used SSA and Hidden Markov Model for bearing fault diagnosis (2013). Muruganatham, Sanjith, Krishnakumar and Murty used SSA to extract bearing fault features and then used ANN for fault classification (2013). Chao and Loh used SSA for structural health monitoring in bridges (2014).

In this paper, a SSA-based envelope analysis is proposed for fault diagnosis of rolling element bearings. The SSA is utilized to decompose the bearing vibration signal into a set of eigentriples, and then a subset of the eigentriples that dominate variation in the original signal is selected to reconstruct a denoised signal. Envelope analysis is then applied to the reconstructed signal to diagnose the bearing faults. The proposed SSA-based envelope analysis is applied to CWRU bearing data sets to demonstrate the effectiveness.

2. METHOD: SSA-BASED ENVELOPE ANALYSIS

2.1. Singular Spectrum Analysis

SSA decomposes a time series into a sum of components, each having a meaningful interpretation. The name "singular spectrum analysis" relates to the spectrum of eigenvalues in singular value decomposition (SVD) of a covariance matrix, and not directly to frequency domain decomposition. The basic SSA algorithm is briefly described as following (Golyandina , N., & Zhigljavsky, 2013):

1. Embedding

To perform the embedding the original time series is mapped into a sequence of lagged vectors of size L by forming ($K = N - L + 1$) lagged vectors:

$$X_i = (x_i, \dots, x_{i+L-1})^T \quad (1 \le i \le K)$$

of size *L*. Thus the *trajectory matrix* of the series **X** is

$$\boldsymbol{X} = [X_i : \dots : X_K] = \left(x_{ij}\right)_{i,j=1}^{L,K} = \begin{pmatrix} x_1 & x_2 & x_3 & \dots & x_K \\ x_2 & x_3 & x_4 & \dots & x_{K+1} \\ x_3 & x_4 & x_5 & \dots & x_{K+2} \\ \vdots & \vdots & \vdots & \ddots & \vdots \\ x_L & x_{L+1} & x_{L+2} & \dots & x_N \end{pmatrix} \quad (1)$$

The lagged vectors X_i are the columns of the trajectory matrix **X**.

The (i,j)th element of the matrix **X** is $x_{ij} = x_{i+j-1}$ which yields that **X** has equal elements on the 'anti−diagonals' $i + j = const$. (Hence the trajectory matrix is a *Hankel matrix*.) Equation (1) defines a one-to-one correspondence between the trajectory matrix of size $L \times K$ and the time series.

2. Singular value decomposition

In this step, the singular value decomposition (SVD) of the trajectory matrix **X** is performed. It decomposes matrix **X** in form

$$\mathbf{X_i} = \sum_{\boldsymbol{i=1}}^{\boldsymbol{d}} \sqrt{\lambda_i} U_i V_i^T \quad (2)$$

where λ_i $(i = 1, \dots, L)$ are eigenvalues of the matrix $\mathbf{S} = \mathbf{X}\mathbf{X}^{\mathrm{T}}$ arranged in order of decrease, $d = \operatorname{rank} \mathbf{X} = \max\{i, \text{such that } \lambda_1 > 0\}$, $\{U_1, \dots, U_L\}$ is the corresponding orthonormal system of the eigenvectors of the matrix **S**, and $V_i = \mathbf{X}^T U_i / \sqrt{\lambda_i}$

3. Eigentriple grouping

The grouping is the procedure of arranging the matrix terms $\mathbf{X_i}$ in Equation (2). It partitions the set of indices {1,…,*d*} into *m* disjoint subsets sets $I_1, \dots, I_m$. The procedure of choosing the sets $I_1, \dots, I_m$ is called eigentriple grouping. If $m = d$ and $I_m = \{j\}$, $j = 1, \dots, d$, then the corresponding grouping is called elementary.

4. Diagonal averaging

In this step, each matrix of the grouped decomposition is transformed into a new series of length N by applying a linear transformation known as diagonal averaging. Let Y be an L×K matrix with elements y_{ij}, $1 \le i \le L, 1 \le j \le K$. Set $L^* = \min(\mathrm{L}, \mathrm{K})$, $K^* = \max(\mathrm{L}, \mathrm{K})$ and $N = L + K - 1$. Let $y_{ij}^* = y_{ij}$ if $L < K$ and $y_{ij}^* = y_{ji}$ otherwise. By making the diagonal averaging the matrix **Y** is transferred into the series $y_1, \dots, y_N$ using the formula

$$y_k = \begin{cases} \dfrac{1}{k} \displaystyle\sum_{m=1}^{k} y_{m,k-m+1}^* & \text{for } 1 \le k < L^* \\ \dfrac{1}{L^*} \displaystyle\sum_{m=1}^{L^*} y_{m,k-m+1}^* & \text{for } L^* \le k \le K^* \\ \left(\dfrac{1}{N-k+1}\right) \displaystyle\sum_{m=k-K^*+1}^{N-K^*+1} y_{m,k-m+1}^* & \text{for } K^* < k \le N \end{cases} \quad (3)$$

Through diagonal averaging, the original time series $\{x_1, \dots, x_N\}$ is decomposed into a sum of m reconstructed series $\{\tilde{x}_1, \dots, \tilde{x}_m\}$.

2.2. Envelope Spectrum based on SSA

Firstly, the vibration data collected from bearing housing is decomposed using SSA. Then, the dominant eigentriples are reconstructed. Thirdly, envelope spectrum analysis is applied to the reconstructed signal to extract the impulse modulation caused by the local faults in bearing. Analysis of the envelope spectrum with the prior knowledge of the

bearing fault frequencies will help to make diagnostic decision. The diagram of the proposed approach is shown in Figure 1.

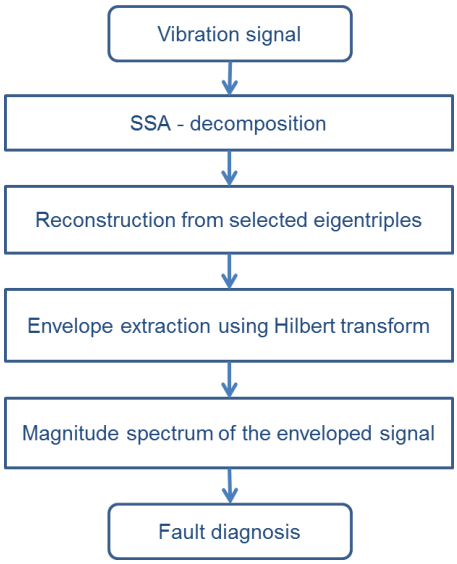

Figure 1. Diagram of the SSA-based envelope analysis.

3. EXPERIMENTAL DATA

In this work, the data sets from the Case Western Reserve University (CWRU) bearing data center are used to validate the effectiveness of the proposed method.

The experimental setup is shown in Figure 2, the test stand consists of a 2 HP motor, a torque transducer/encoder, a dynamometer, and control electronics. The test bearings support the motor shaft. Single point faults were introduced to the test bearings using electro-discharge machining with fault diameters of 0.18 mm, 0.36 mm, 0.53 mm, 0.71 mm (i.e., 7 mils, 14 mils, 21 mils, 28 mils, and 40 mils) and a depth of 0.28 mm. Vibration data was collected using accelerometers from the housing. Digital data was collected at 12 kHz for the fan end bearing and 48 kHz for drive end bearing. In order to quantify this effect, experiments were conducted for both fan and drive end bearings with outer raceway faults located at 3 o'clock (directly in the load zone), at 6 o'clock (orthogonal to the load zone), and at 12 o'clock. More details about the experiments and the data can be found at CWRU bearing data center website and the review paper by Wade and Randall (2015).

In this work, the drive end bearing fault data sampled at 48 kHz are used. The drive end bearing is SKF 6205-2RS JEM deep groove ball bearing and its specifications are listed in Table 1. The corresponding bearing fault frequencies are listed in Table 2 (ratios to the shaft frequency).

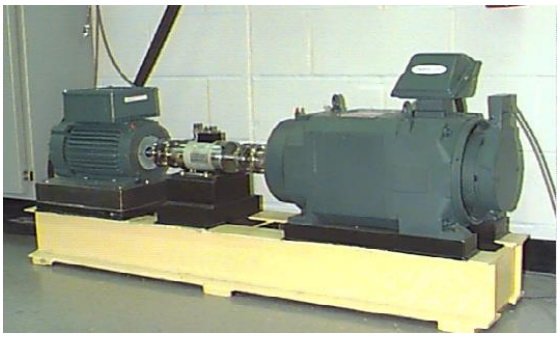

Figure 2. CWRU bearing test rig.

Table 1. Specification of the drive end bearing

Parameter	Dimension (mm)
Inside diameter	25.001
Outside diameter	51.999
Thickness	15.001
Ball diameter	7.940
Pitch diameter	39.040

Table 2. Bearing fault frequencies (drive end)

Faulty component	Ratio to shaft rotating frequency
Inner race (BPFI)	5.415
Outer race (BPFO)	3.585
Cage train (FTF)	0.398
Rolling element (BFF)	4.714

4. FAULT DIAGNOSIS USING SSA-BASED ENVELOPE ANALYSIS

4.1. Window Length for SSA

The window length L is the main parameter of SSA. Adequate choice of L enables grouping activity leading to a good SSA decomposition. The variations in L may influence both weak and strong separability features of SSA. There are several general principles for the selection of the window length L that have certain theoretical and practical grounds. The common recommendation on choice of L is $L \cong N/2$ for a time series with length of N to achieve the most detailed decomposition (Golyandina & Zhigljavsky, 2013). However, it not necessary to use such a large value of the window length L for mechanical vibration signals. For most of the mechanical vibration signals, L = 20 is sufficient. Figure 3 (a) shows a singular spectrum decomposition of a vibration signal collected from a gearbox (PHM Challenge 2009 Data Sets). The first 9 eigentriples retained more than 99% norm of the trajectory

matrix. Figure 3 (b) shows a singular spectrum decomposition of a vibration signal from the CRWU data sets, and the first 6 eigentriples retained more than 99% norm of the trajectory matrix.

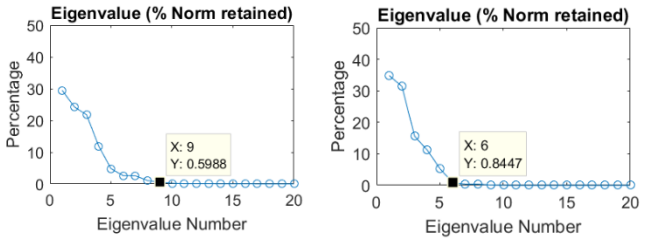

(a) (b)

Figure 3. Singular spectrum of mechanical signals

4.2. Selection of eigentriples for Reconstruction

In addition to the choice of the window length for SSA, another important thing is that how many eigentriples should be used for reconstruction for a real application. In general, selection of eigentriples that retain more than 75% norm of the trajectory matrix is sufficient to reconstruct the signal (Kilundu, Chiementin, & Dehombreux, 2011). Zhao and Ye (2011) proposed an approach called difference spectrum for selection of effective eigentriples for SSA reconstruction and applied it to fault diagnosis of headstock. Sometimes the difference spectrum is not reliable for SSA reconstruction as it may only retain less than 50% of the norm of the trajectory matrix. In the singular spectrum shown in Figure 3 (b), the difference spectrum recommends to select the first two eigentriples which retain about 66% of the norm of the trajectory matrix. In this work we adopt the criteria of retaining 75% norm of the trajectory matrix.

Figure 4 shows a singular spectrum decomposition of a vibration signal from the CRWU data sets (109.mat, inner race fault). Figure 5 shows the reconstruction using the first two eigentriples (66% norm retained), the comparison with the original signal, and the residual. Figure 6 shows the reconstruction using the first three eigentriples (82% norm retained), the comparison with the original signal, and the residual.

Figure 7 shows a singular spectrum of another bearing vibration signal (135.mat, outer race fault at 6 o'clock location). The first two eigentriples account more than 95% norm of the trajectory matrix. Figure 8 shows the reconstruction using the first two eigentriples (95% norm retained), the comparison with the original signal, and the residual. It can be seen that the reconstruction with the first two eigentriples is almost coincided with the original signal.

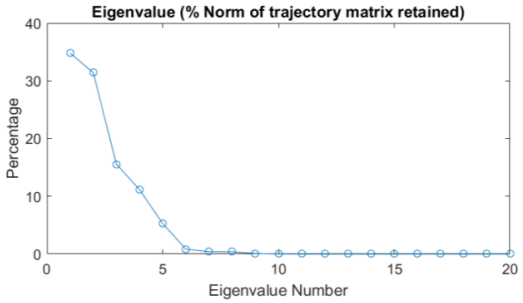

Figure 4. Singular spectrum of bearing data (109.mat)

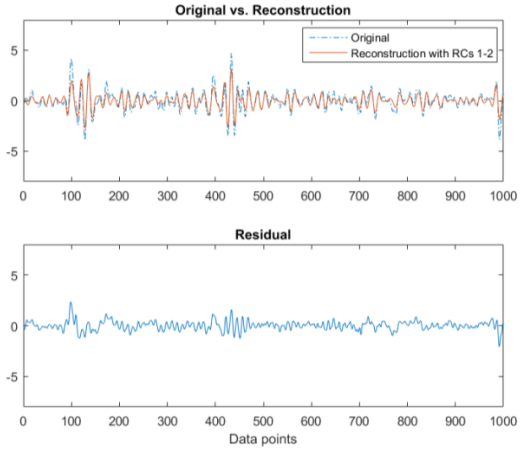

Figure 5. Reconstruction using the first two eigentriples (66% norm retained) and the residual (109.mat)

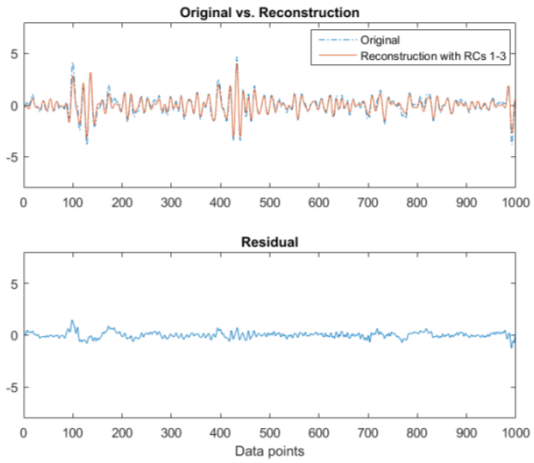

Figure 6. Reconstruction using the first three eigentriples (82% norm retained) and the residual (109.mat)

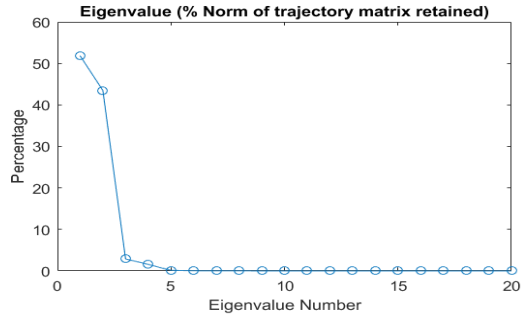

Figure 7. Singular spectrum of bearing data (135.mat)

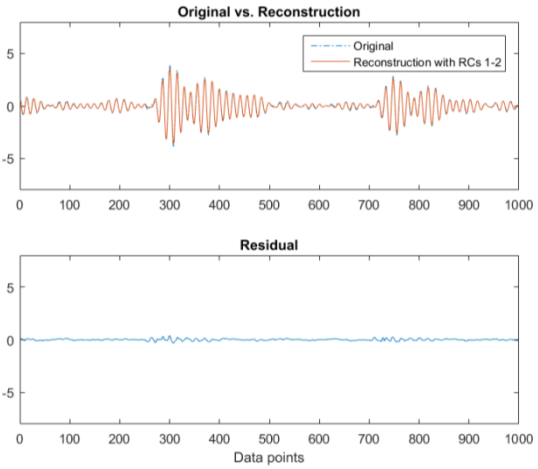

Figure 8. Reconstruction using the first two eigentriples (95% norm retained) and the residual (135.mat)

4.3. Bearing vibration data analysis

In this section, the data sets from the Case Western Reserve University (CWRU) bearing data center are used to demonstrate the effectiveness of the proposed approach. The diagnostic results are compared with that of the well-developed Kurtogram approach (Antoni & Randall, 2006). Usually, the dominant components in the envelope spectrum of rotating machinery are the shaft frequency and its harmonics. The modulation caused by the faulty bearing components is often masked by the strong shaft rotating related components. This can be seen from the envelope spectrum shown in Figure 11. If the modulation information is properly extracted, it should be seen from the envelope spectrum the fault frequencies, i.e., Ball Pass Frequency of Inner race (BPFI) for inner race fault, Ball Pass Frequency of Outer race (BPFI) for outer race fault, Fundamental Train Frequency (FTF) for cage fault and Ball Fault Frequency for rolling element fault, as shown in Table 2 .

In order to quantitatively describe the effectiveness of the approaches, an index r is defined as the ratio between the magnitudes of the fault frequency A_f and the shaft frequency A_s: $r = A_f/A_s$. Larger r value means more effective.

4.3.1. Case 1: Inner Race Fault

Figure 9 shows a time domain signal of bearing inner race fault (data file: 109.mat). The motor speed is 1797 rpm, thus the shaft frequency is $f_r = 1797/60 = 29.95$ Hz. The feature frequency for the inner race fault is $BPFI = 5.415 \times 29.95 = 162.1$ Hz (refer to Table 2 for the BPFI ratio). Figure 10 shows the band-pass filtered signal based on Kurtogram identified resonance band. It can be seen that it is very impulsive due to the modulation by the shaft frequency. This can be more clearly seen from the envelope spectrum shown in Figure 11. From the envelope spectrum it is seen that the dominant components are the shaft frequency (around 30 Hz) and its harmonics. The fault frequency BPFI (161.9 Hz) can also be seen but the magnitude is very small. In this case, the effectiveness ratio: $r = 0.21$.

Figure 12 shows the reconstructed signal using the first three eigentriples (82% norm of the trajectory matrix retained, which is greater than 75%). Figure 13 shows the envelope spectrum of the reconstructed signal shown in Figure 12. It is seen that the magnitude of the fault frequency becomes much higher than that of the shaft frequency. Here the effectiveness ratio: $r = 21.98$.

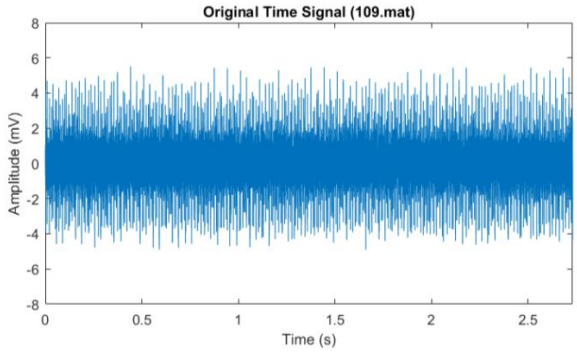

Figure 9. Time signal of bearing inner race fault

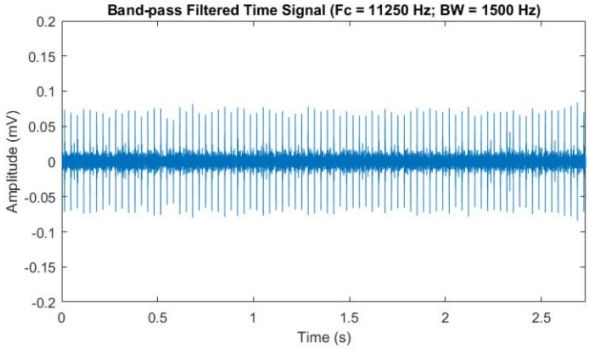

Figure 10. Band-pass filtered signal based on Kurtogram approach

Figure 14 shows the envelope spectrum of the reconstructed signal using the first six eigentriples (99% norm of the trajectory matrix retained). The envelope spectrum looks very similar with the envelope spectrum shown in Figure 13, and the effectiveness ratio: $r = 36.25$ which is larger than that of the envelope spectrum shown in Figure 13. However, it is quite obvious that reconstruction using the first three eigentriples which retaining more than 75% norm of the trajectory matrix is good enough for envelope detection.

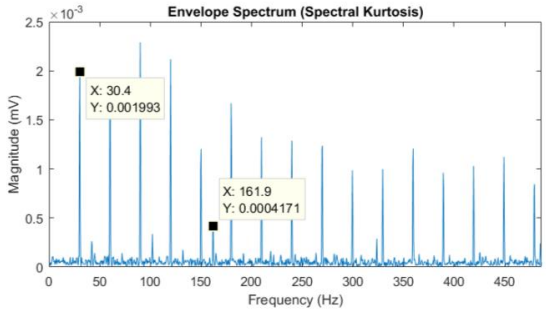

Figure 11. Envelope spectrum based on Kurtogram approach

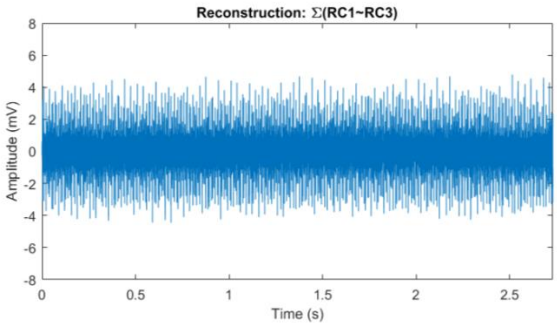

Figure 12. Reconstructed signal (RC 1~3, 82% norm retained)

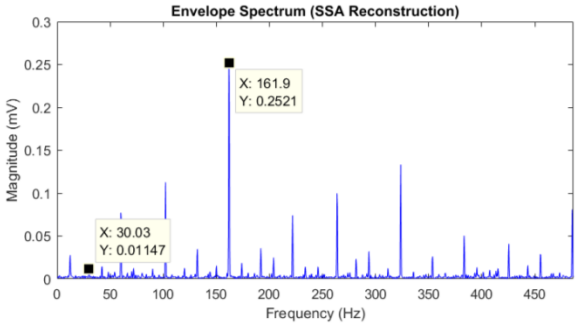

Figure 13. Envelope spectrum of SSA reconstruction (RC 1~3, 82% norm retained)

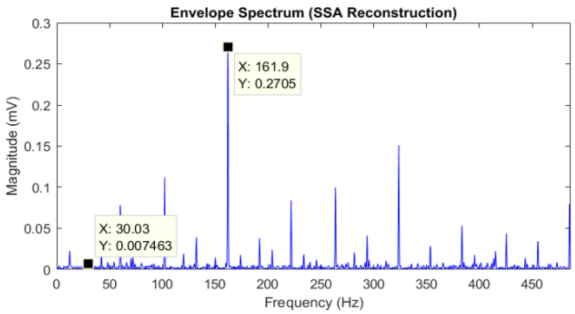

Figure 14. Envelope spectrum of SSA reconstruction (RC 1~6, 99% norm retained)

4.3.2. Case 2: Outer Race Fault

Figure 15 shows the time domain signal of bearing outer race fault (data file: 135.mat). The motor speed is about 1797 rpm, thus the shaft frequency is $f_r = 1797/60 = 29.95$ Hz. The feature frequency for the inner race fault is $BPFO = 3.5848 \times 29.95 = 107.4$ Hz. Outer race is stationary and the fault on it is relatively easier to diagnose comparing the fault on inner race. Figure 16 shows the band-pass filtered signal based on Kurtogram identified resonance band.

Figure 17 shows the envelope spectrum of the band-pass filter signal. In this case, the fault frequency (108 Hz) and its harmonics are quite clearly shown in the envelope spectrum. The effectiveness ratio is: $r = 2.41$.

Figure 18 shows the SSA reconstructed signal using the first two eigentriples (95% norm of the trajectory matrix retained). Figure 19 shows the envelope spectrum corresponding to the reconstructed signal shown in Figure 18. The effectiveness ratio is: $r = 6.45$, which is also significantly larger than that of the envelope analysis based on Kurtogram.

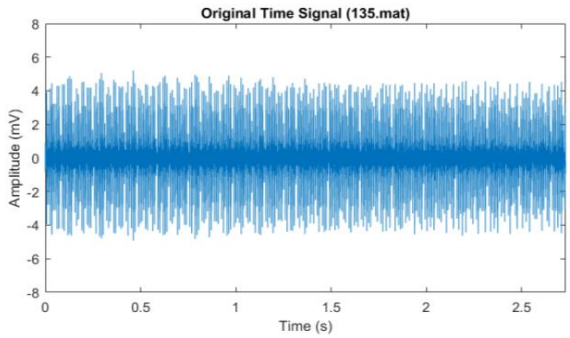

Figure 15. Time signal of bearing outer race fault signal

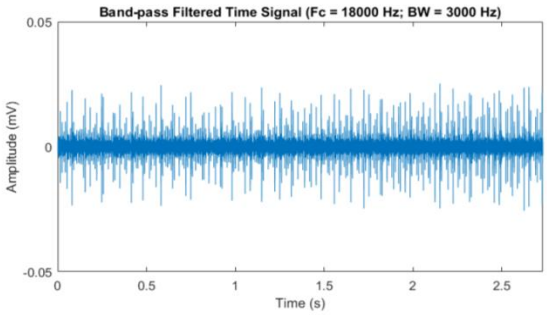

Figure 16. Band-pass filtered signal based on Kurtogram approach

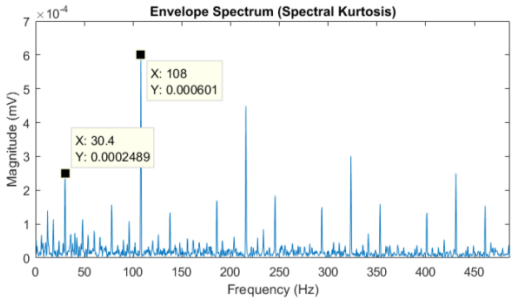

Figure 17. Envelope spectrum based on Kurtogram approach

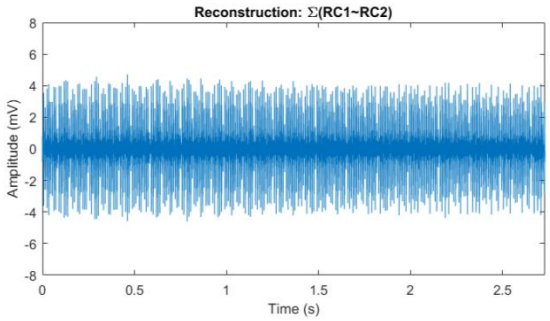

Figure 18. Reconstructed signal (RC 1~2, 95% norm retained)

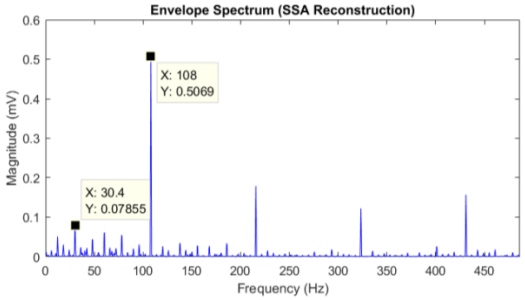

Figure 19. Envelope spectrum of SSA reconstruction

5. CONCLUSION

In this paper, singular spectrum analysis is applied to decomposition and reconstruction of bearing vibration signals as a preprocessing approach. The envelope analysis is then applied to the reconstructed signal using the selected eigentriples (principle components) to extract the modulation information caused by faulty bearing components. The results of the SSA-based envelope analysis are compared with the widely used Kurtogram-based envelope analysis. The results show that the proposed approach is more effective than the Kurtogram-based envelope analysis.

REFERENCES

Alharbi, N., & Hassani, H. (2016). A new approach for selecting the number of the eigenvalues in singular spectrum analysis. *Journal of the Franklin Institute* vol. 353. pp. 1–16. doi: 10.1016/j.jfranklin.2015.10.015

Antoni, J. (2006). The spectral kurtosis: application to the vibratory surveillance and diagnostics of rotating machines. *Mech. Syst. Signal Process*. Vol. 20, pp. 282-307. doi:10.1016/j.ymssp.2004.09.001

Antoni, J., & Randall R. B. (2006). The spectral kurtosis: a useful tool for characterising non-stationary signals. *Mech. Syst. Signal Process*. Vol. 20, pp. 308-331. doi:10.1016/j.ymssp.2004.09.002

Bearing Data Centre, Case Western Reserve University, Available: http://csegroups.case.edu/bearingdatacenter/home

Broomhead, D.S., & King, G.P. (1986). Extracting qualitative dynamics from experimental data. Physica D. vol. 20, pp. 217–236. doi: 10.1016/0167-2789(86) 90031-X

Chao, S.-H. & Loh, C.-H. (2014). Application of singular spectrum analysis to structural monitoring and damage diagnosis of bridges. *Structure and Infrastructure Engineering: Maintenance, Management, Life-Cycle Design and Performance*, vol. 10:6, pp. 708-727, doi: 10.1080/15732479.2012.758643

Golyandina , N., & Korobeynikov, A. (2014). Basic Singular Spectrum Analysis and forecasting with R. *Computational Statistics & Data Analysis*, vol. 71, pp. 934-954. doi: 10.1016/j.csda.2013.04. 009

Golyandina, N., & Zhigljavsky, A. (2013). *Singular Spectrum Analysis for Time Series*. Springer. Doi: 10.1007/978-3-642-34913-3

Harris, T.J., & Yuan, H. (2010). Filtering and frequency interpretations of Singular Spectrum Analysis. *Physica D* vol. 239, pp. 1958–1967. doi:10.1016/j.physd. 2010.07.005

Hassani, H. (2010). Singular spectrum analysis based on the minimum variance estimator. *Nonlinear Analysis: Real World Applications*, vol. 11, pp. 2065–2077. doi: 10.1016/j.nonrwa.2009.05.009

Khan, M. A. R., & Poskitt, D. S. (2013). A note on window length selection in singular spectrum analysis. *Australian & New Zealand Journal of Statistics.* vol. 55(2), pp. 87–108. doi: 10.1111/anzs.12027

Khelifa, S., Kahlouche, S., & Belbachir, M. F. (2012). Signal and noise separation in time series of DORIS station coordinates using wavelet and singular spectrum analysis. Comptes Rendus Geoscience, vol. 344, pp. 334-348., doi: 10.1016/j.crte.2012.05.003

Kilundu, B., Chiementin, X., & Dehombreux, P. (2011). Singular spectrum analysis for bearing defect detection. *Journal of Vibration and Acoustics*, Vol. 133(5), pp. 051007-051007-7. doi: 10.1115/1.4003938

Kilundu, B., Dehombreux, P. & Chiementin, X. (2011). Tool wear monitoring by machine learning techniques and singular spectrum analysis. Mech. Syst. Signal Process, vol. 25, pp. 400–415 doi:10.1016/j.ymssp. 2010.07.014

Liu, T., Chen, J. & Dong, G. M. (2013). Singular spectrum analysis and continuous hidden Markov model for rolling element bearing fault diagnosis. *Journal of Vibration and Control*, vol. 21(8). pp. 1506-1521. doi: 10.1177/1077546313496833

Muruganatham, B., Sanjith, M.A., Krishnakumar, B., & Murty, S.A.V. S. (2013). Roller element bearing fault diagnosis using singular spectrum analysis. *Mech. Syst. Signal Process*, vol. 35, pp. 150–166. doi: 10.1016/j. ymssp.2012.08.019

PHM Challenge 2009 Data Sets: http://www.phmsociety.org/references/datasets

Randall R. B., & Antoni, J. (2011). Rolling element bearing diagnostics – A Tutorial. *Mech. Syst. Signal Process*. Vol. 25, pp. 485-520. doi:10.1016/j.ymssp.2010.07.017

Salgado, D.R., & Alonso, F.J. (2006). Tool wear detection in turning operations using singular spectrum analysis. Journal of Materials Processing Technology, vol. 171, pp. 451–458. doi:10.1016/j.jmatprotec.2005.08.005

Sanei, S., & Hassani, H. (2016). *Singular spectrum analysis of biomedical signals*. CRC Press, Taylor & Francis Group.

Viljoen, H. & Nel, D.G. (2010). Common singular spectrum analysis of several time series. Journal of Statistical Planning and Inference vol. 140, pp. 260-267. doi:10.1016/j.jspi.2009.07.009

Shi, D.F., Wang W. J., & Qu, L. S.(2004). Defect Detection for Bearings Using Envelope Spectra of Wavelet Transform. *J. Vib. Acoust*, 126(4), pp. 567-573. doi:10.1115/1.1804995

Smith, W. A., & Randall R. B. (2015). Rolling element bearing diagnostics using the Case Western Reserve University data: A benchmark study. *Mech. Syst. Signal Process*. Vol. 64-65, pp. 100-131. doi: 10.1016/j.ymssp. 2015.04.021

Vautard, R. & Ghil, M. (1989). Singular spectrum analysis in nonlinear dynamics, with applications to paleoclimatic time series. *Physica D*, Vol. 35(3), pp. 395-424. doi: 10.1016/0167-2789(89)90077-8

Wade A. Smith, W.A., & Randall, R.B. (2015). Rolling element bearing diagnostics using the Case Western Reserve University data: A benchmark study. *Mech. Syst. Signal Process*, vol. 64–65, pp. 100–131. doi: 10.1016/j.ymssp.2015.04.021

Wang, D., Tse, P. W., & Tsui, K. L. (2013). An enhanced Kurtogram method for fault diagnosis of rolling element bearings. *Mech. Syst. Signal Process*, vol. 35, pp. 176-199. doi: 10.1016/j.ymssp. 2012.10.003

Zhao, X. Z. & Ye, B.Y. (2011). Selection of effective singular values using difference spectrum and its application to fault diagnosis of headstock. *Mech. Syst. Signal Process*, vol. 25, pp. 1617-1631. doi:10.1016/j.ymssp. 2011.01. 003

BIOGRAPHIES

Guicai Zhang received the M.S. from Xi'an JiaoTong University, Xi'an, China in 1993, the Ph.D. from Huazhong University of Science and Technology, Wuhan, China in 2000, both in Mechanical Engineering. He is a Staff Research Engineer in the area of prognostics and health management and intelligent manufacturing at United Technologies Research Center (China). Before joining United Technologies Research Center (China) in 2005, he was an Associate Professor at Shanghai JiaoTong University from 2003 to 2005 and Research Associate at the Chinese University of Hong Kong from 2000 to 2003. He published over 30 papers in peer-reviewed journals and international conferences. He is a Council Member of Shanghai Vibration Engineering Society and a Senior Member of China Mechanical Engineering Society.

Yun Li received the M.S. from Shanghai JiaoTong University, Shanghai, China in 2007, the MBA from Tongji University, Shanghai, China in 2012. He is a Staff Research Engineer who is leading innovative technologies development of building HVAC and refrigeration system diagnostics and data analytics at United Technologies Research Center (China).

Changle Li holds Doctorate degree in mechanics from Universite Lille 1 in France in 2004. He has Master of Science and Bachelor of Science degrees in engineering mechanics from Tsinghua University, Beijing. Before joining UTRC, he worked at Saint-Gobain in France and China for 10 years. He joined United Technologies Research Center (China) in 2013 as Group Leader, Mechanical Systems. He is currently project leader for OTIS program office at United Technologies Research Center (China).